

---

**REVIEW**

---

**The Electrospray and Combustion at the Mesoscale<sup>†</sup>**Sebastian KAISER,<sup>a)</sup> Dimitrios C. KYRITSIS,<sup>a), b)</sup> Peter DOBROWOLSKI,<sup>a)</sup>  
Marshall B. LONG,<sup>a)</sup> and Alessandro GOMEZ<sup>\*a)</sup>

(Received November 5, 2002; Accepted November 11, 2002)

An application of the electrospray to mesoscale combustion is studied, with the ultimate goal of coupling the combustor with direct energy conversion modules for power production. The combustor design relies on fuel dispersion by multiplexed electrosprays coupled with a series of catalytic meshes acting as ground electrode and initiators of the fuel oxidation. The combustor has a volume on the order of few cm<sup>3</sup> and operates on jet fuel (JP 8), which is electrosprayed at a flow rate on the order of 10 g/h with equivalence ratios varying from 0.35–0.70. The behavior of the electrospray in high temperature environments is examined and the phenomenology of the electrospray in the combustion chamber is visualized using planar laser-induced fluorescence from a fluorescent tag doped into the fuel. Combustion efficiencies on the order of 97% can be achieved with uniform temperatures at the catalyst in the range of 900–1,300 K (within  $\pm 5\%$ ) when the electrospray is operated in an unsteady mode, accompanied by a “hissing” sound characteristic of the onset of corona discharge. Remarkably, no fouling, soot, or NO<sub>x</sub> were detected in the exhaust gases, which resulted in clean and efficient combustion of even environmentally problematic liquid hydrocarbons.

**1. Introduction**

An inevitable prerequisite to the successful combustion of liquid fuels is their dispersion in a typically gaseous oxidizer. The goal is to maximize the combustion efficiency while minimizing pollutant formation by achieving as intimate a mixing of the reactants as possible. Several atomization techniques have been used in the past, most of them reviewed by Lefevbre.<sup>1)</sup> Not much emphasis has been given to electrostatic means of atomization. Yet, an electrostatic spray (ES) offers several advantages compared to alternative atomization techniques. In its simplest configuration, which is the one used in this work, a semi-conducting liquid emerging from the tip of a capillary tube is charged to a sufficiently high potential with respect to a ground electrode a short distance away, so that the liquid meniscus takes the shape of a cone from the tip of which a thin liquid thread emerges. This microjet breaks into a stream of charged droplets, which eventually spread to form a spray; more properly, an electrospray. Cloupeau and Prunet-Foch<sup>2)</sup> give a comprehensive account of the phenomenology of the various modes of operation. Following these authors, we refer to the ES configuration employed in this study as the cone-jet mode. Numerous features distinguish the electrospray from other atomization techniques:

- i) it may consist of quasi-monodisperse droplets, the size of which can be varied over a very broad range (1–200  $\mu\text{m}$ )<sup>3)</sup>;
- ii) these droplets are generated from capillaries or orifices with a relatively large bore with respect to the size of the generated droplets, which implies that clogging risks are minimized;
- iii) the Coulombic repulsion of the charged droplets induces spray self-dispersion and prevents droplet coalescence;
- iv) the atomization which is strictly electrostatic is decoupled from gas flow processes, providing some flexibility in the selection and control of the experimental conditions;
- v) the presence of electric charge on the droplets allows, in principle, for some control of their trajectories by electrostatic fields.

The electrospray has initiated a veritable revolution in the area of mass spectrometry, spearheaded by the pioneering work of John B. Fenn at Yale in the 80's. Applications to other areas have been hampered by the low flow rates at which the cone-jet mode can be established. Specific to combustion, Thong and Weinberg<sup>4)</sup> obtained remarkably monodispersed droplets using an electrospray operated in the cone-jet mode and reported the feasibility of burning such spray in a counter-flow premixed flame at a flow rate of about 0.5 mL/min, a value that is typical of liquid fuel electrosprays. Such flow rates have been traditionally regarded as too small for any technological application, but large enough for laboratory scale experiments.<sup>5)</sup>

This state of affairs changed recently, when combustion became attractive for small-scale power generation, because of the large power density (power/

---

\*a) *Yale Center for Combustion Studies, Department of Mechanical Engineering, Yale University (New Haven, CT 06520–8286, USA)*

Fax: (203) 432–7654, e-mail: [alessandro.gomez@yale.edu](mailto:alessandro.gomez@yale.edu)

b) *Current address: Department of Mechanical and Industrial Engineering, University of Illinois (Urbana-Champaign, IL, USA)*

---

<sup>†</sup> **Congratulations on winning the 2002 Nobel Prize**

Contributed to a Special Issue of the *Journal of the Mass Spectrometry Society of Japan* (JMSSJ) in honor of John B. Fenn, 2003.

volume) offered by liquid fuels, up to two orders of magnitude larger than the best batteries available on the market today. Combustion at a small scale is being considered for a variety of applications, including: micro-heat engines, as readily rechargeable batteries for electric power generation; miniaturized internal combustion engines for the propulsion of micro-air vehicles; micro-thrusters to power small satellites impulsively, an application in which it competes with the direct use of the electro spray in ion propulsion; or to launch and power “smart dust,” airborne micro-sensors connected by a wireless network. The power requirements of all these applications are on the order of tens or hundreds of Watts, with the overall dimension of the device of, at most, a few cm.

Liquid fuel combustion can be implemented after the liquid fuel has been either pre vaporized or sprayed. A suitable choice in the first case is an evaporator, extracting heat from the combustion flue gases. However, one potential difficulty using some of the heavy fuels of interest is that the fuel may decompose thermally in the presence of hot surfaces, in which case carbon-based deposition, fouling and plugging of the micro-channels may ensue. The problem is particularly severe at the location where the phase change occurs and is affected by the residence time.<sup>6)</sup> The alternative to pre-evaporation is dispersing the fuel using an electro spray technique, probably the only viable approach to burn directly minute amounts of liquid hydrocarbons. Critical to uniform evaporation and burning is a good control of the size distribution of the resulting aerosol, which can be achieved by operating the electro spray in the so-called cone-jet mode. This capability would ensure uniformity of evaporation and burning time, an important feature of an optimally miniaturized microcombustor.

Miniaturized combustors can be realized using the same micro-fabrication techniques that have been developed for the electronics industry. These techniques easily lend themselves to mass production, which has been a key factor in the extraordinary growth of the electronics industry in the last few decades. As a result, if the promise of miniaturized combustion is demonstrated, economies of mass production may replace economies of scale. Consider the analogous situation in which the introduction of the “microPC” was accepted with skepticism two decades ago by the scientific community, as some kind of sophisticated typewriter. Yet, properly networked, a few years later PCs could even compete with, and often replace, mainframes. A program on small scale combustion would lead to the development of the ultimate distributed power source. Charging, say, a laptop the same way as a cigarette-lighter, without being hampered by short-lived and heavy batteries, could be a reality in the not too distant future.

Since this article was written for a book in honor of John B. Fenn, one of the authors (AG) feels compelled to acknowledge the inspirational role that Professor Fenn played in exposing him at the beginning of his academic career to the virtues of the electro spray. Fenn’s contagious enthusiasm, creativity and intellectual longevity make him an example that we can only hope to

emulate. It is the authors’ hope that mesoscale combustion applications of the electro spray follow the fate of electro spray ionization, despite Fenn’s misgivings about the wisdom of applying such a promising technology to a seemingly mature field like combustion.

## 2. Combustor Design Considerations

For micro-combustion to be competitive, energy conversion must be achieved by adapting the same inexpensive and ubiquitous fuel supply of conventional combustion, that is, liquid hydrocarbons. Among the latter, JP8 is the fuel of choice in many applications, because of its availability as automotive and aviation fuel. JP8 consists of a mixture of paraffin, naphthene and aromatic hydrocarbons. Such a fuel presents the greatest challenge from an environmental point of view, being a mixture of heavy hydrocarbons, the clean burning of which is very difficult. The emphasis is on burning JP8 cleanly and efficiently in as small a chamber as possible and extracting some of the thermal energy from the combustion process using simple energy conversion processes and a minimum of moving parts.

### 2.1 Multiplexing and premixed catalytic oxidation

Since the size of the generated droplets and, consequently, the droplet evaporation time are monotonic functions of the liquid flow rate, it is best to multiplex the electro spray and use a system of several capillaries mounted in parallel. This approach would also help in achieving a reasonably uniform temperature in the combustor cross-section, which is important for subsequent thermal-to-electrical energy conversion.

Rather than igniting in the vicinity of the electro spray source, one could ignite farther downstream after substantial mixing with the oxidizer has occurred, using a gauze or honeycomb to separate the combustion region from the electro spray and to prevent flashback. This premixed alternative was explored decades ago in some pioneering work by Weinberg.<sup>4)</sup>

The likelihood of short residence times in the combustor may create significant emissions of CO, and probably, unburned hydrocarbons, in which case catalytic combustion strategies would be particularly promising. Catalytic combustion offers not only emission advantages, but also stability benefits and appears to be a natural choice for mesoscale combustion. Particularly well-suited for small scale applications is a recently developed catalyst substrate design (Microlith<sup>®</sup>)<sup>7)</sup>. It consists of a number of catalytically coated grids or screens stacked serially, each with short channel lengths, high cell density and low thermal mass. The resulting reactor is very compact, has rapid transient response and high energy density, and requires small loadings of precious metal catalysts. Catalyst formulations have been selected from platinum group metals and an alumina washcoat with appropriate additives. The advantages of this design stem from the reduction in mass transfer limitations, as compared to conventional monoliths having relatively thick boundary layers. Also, under conditions of kinetic control, the particular design can pack more active area into a small volume, which means that insertion of such cata-

lysts in a flow can provide more effective fuel conversion for a given pressure drop.

With these considerations in mind, we designed a combustor consisting of a system of multiplexed electrospays for the liquid fuel dispersion in which a series of catalytic Microliths a few centimeters downstream acted as the ground electrode. The objective of the electro spray based fuel delivery system is to produce a lean, uniform mixture of fuel and air upstream of the catalyst. Combustion is initiated at the catalyst and probably continues in the gas phase. Then, complete combustion can be achieved (*i.e.* minimal unwanted emissions) and a uniform surface temperature in the range 900–1,300 K can be established for subsequent coupling with direct energy conversion modules (*e.g.*, thermoelectric generation (TEG), or thermophotovoltaic (TPV)). In the remainder of this contribution, we discuss the operation of such a system, as first reported in ref. 8, and we focus on the behavior of the electro spray in these high temperature systems.

### 3. Experimental System

#### 3.1 Burner

A schematic of the experimental burner is shown in Fig. 1. The fuel, JP8 doped with 0.05% per mass of a proprietary antistatic additive (Stadis 450, Du Pont) to enhance its electric conductivity, was metered with a syringe pump. The flow was distributed through a poly-ether-ether-ketone (PEEK) manifold into 19 stainless steel capillaries (1.59 mm o.d., 127  $\mu\text{m}$  i.d., 10 cm length) arranged in a hexagonal pattern with two concentric hexagons surrounding the central capillary. The capillaries were mounted through a teflon flange and their tips were sharpened and polished to eliminate burrs that would affect the electric field pattern. The flange supported a cylindrical pyrex chamber 38.1 mm in i.d. and 38.1 mm in height that provided optical access. Air was admitted to the chamber at a temperature of 200°C to simulate recuperation in a real device. The chamber was capped at the top with a metal holder in which three Microlith<sup>®</sup> catalyst screens were housed. The catalyst was based on a proprietary Pt/Pd

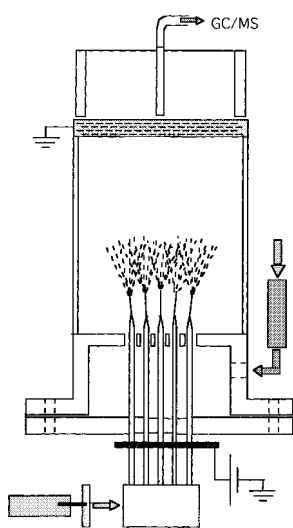


Fig. 1. Schematic of the catalytic mesoscale burner operating with electro sprayed JP8 fuel.

formulation. Each screen was an approximately orthogonal grid of 125  $\mu\text{m}$  wires with 1 mm pitch. Once the capillaries were charged to a voltage on the order of several kV relative to the grounded catalyst, several electrospays were simultaneously established at the capillary tips. The pressure loss across the capillaries was approximately 20 cm of water ( $\sim 2$  kPa) whereas the corresponding pressure drop across the catalyst grid was so small that it could not be measured accurately ( $< 1$  kPa). The current carried by the sprays was measured to be on the order of 100 nA, which yielded a parasitic loss of less than 1 mW for approximately 100 W of thermal power. Fuel atomization, dispersion and vaporization as well as mixing with the coflowing air stream occurred in the cylindrical chamber while combustion was established at or near the catalytic grids.

#### 3.2 Laser diagnostic system

To visualize the fuel distribution in the operating device, planar laser-induced fluorescence (PLIF) of a fuel tracer was used. Fuel PLIF has been used in sprays and combustion devices both qualitatively and quantitatively.<sup>9</sup> In LIF experiments, a molecular transition is excited by the laser. The molecule relaxes to the ground state via fluorescence or quenching by collision with other molecules. In PLIF a laser sheet from a pulsed laser at a suitable wavelength provides excitation, and a camera images the fluorescence. Because the laser pulse and fluorescence decay times are typically shorter than the flow time scales and the signal is relatively strong, instantaneous measurements with a single shot are possible.

As a tracer, 5% of 1-methylnaphthalene was added to the fuel surrogate (*n*-dodecane). The boiling points of tracer and fuel (240°C and 216°C, respectively) were sufficiently close for the tracer to follow the fuel in its evaporation behavior. In addition, naphthalenes typically make up about 5% of the target fuel JP8. The fluorescence decay time for this tracer is on the order of 100 ns. For a chemically similar tracer, toluene, it has been shown that, since oxygen is practically the only effective quencher, the fluorescence signal is essentially proportional to the local equivalence ratio (or fuel/air ratio).<sup>10</sup> The equivalence ratio is defined as the fuel/air ratio on a molar basis normalized to the stoichiometric value. Although we have not verified that this is also the case for 1-methylnaphthalene under the conditions in the evaporation chamber, for qualitative imaging we will assume it to be true. A quantitative investigation of this and the temperature dependence of the fluorescence, which is also not addressed here, is currently under way.

The burner used for diagnostics was slightly modified in that a square geometry, consisting of four fused silica windows pushed together by a Teflon base, is used. This modification allowed for easier optical access without the reflections and distortion that the cylindrical geometry would introduce, and for easier cleaning of the windows. The bottom of the burner containing the holes for the needles and air feed consisted of a ceramic to be able to withstand the heat load from the catalyst radiation. The influence of geometry and materials on the electric field has to be kept in mind, though, and is not always negligible. For exam-

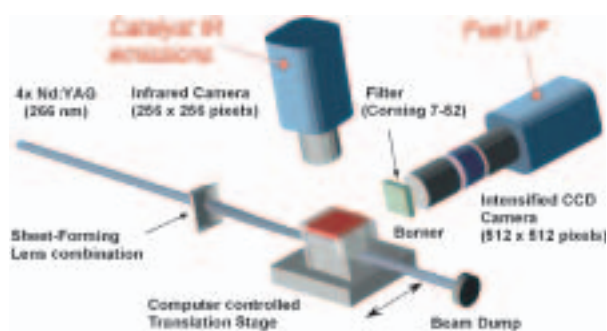


Fig. 2. Experimental arrangement for fuel-tracer PLIF in the burner evaporation chamber.



Fig. 3. Atomization pattern for electro spraying of JP8 into ambient air conditions.

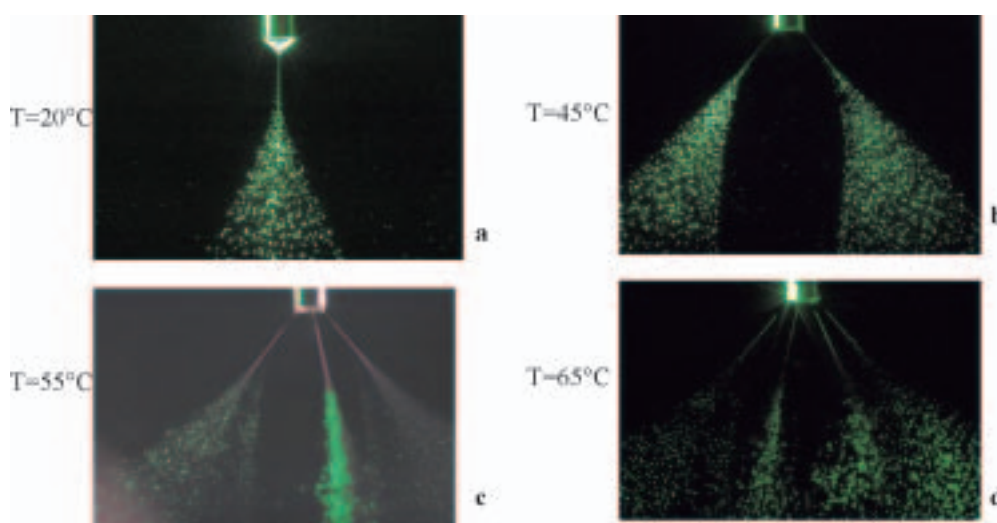


Fig. 4. Ethanol electro spray phenomenology at elevated temperatures.

ple, it was observed that consistently higher voltages were necessary to achieve the same mode of operation as in the “standard” configuration described in the previous section. In addition to the usual intake for heated air the burner also had a port for unheated propane. Before operation with liquid fuel the diagnostics burner was run on propane, by providing a clean heating phase. Switching the burner to liquid fuel when it was hot avoided fouling from fuel condensing on the cold windows. In this way the burner could be operated 30–60 minutes before image degradation becomes intolerable.

The experimental arrangement is shown in Fig. 2. Excitation is provided by the fourth harmonic of an Nd:YAG laser (Continuum Powerlite) with a wavelength of 266 nm, a pulse duration of  $\sim 10$  ns, and a repetition rate of 10 Hz. A combination of spherical and cylindrical lenses forms a vertical sheet of suitable dimensions ( $\sim 18.5$  mm high and 0.5 mm thick) in the evaporation chamber. The burner is mounted on a motorized computer-controlled translation stage such that the entire volume of the chamber can be scanned. Fluorescence occurs broadband in the 330–380 nm range and is detected by an image-intensified CCD camera (Photometrics  $512 \times 512$  pixels lens-coupled to

19 mm DEP MCP intensifier). Scattered laser radiation and longer-wavelength fluorescence of dirt accumulating on the windows is suppressed by a band pass colored glass filter (Corning 7-52); the short gating time of the intensifier (200 ns) avoids interference from the catalyst luminescence. Also shown in the schematic is an infrared-sensitive camera that is used to image the catalyst temperature.

#### 4. Results and Discussion

The mechanism of electro spray atomization of liquid hydrocarbons was studied in detail for isolated electro sprays.<sup>11)</sup> Because of space charge effects, the results of such studies are only of qualitative validity when multiplexed sprays are considered. The appearance of these sprays for JP8 injection is shown in the photograph of Fig. 3, which was taken in room-temperature air so that the relevant structure was clearer. A cone of liquid fuel was formed on each capillary tip from which a short fluid ligament protruded. Atomization was achieved through the breakup of these ligaments, and the Coulombic repulsion among droplets of different sprays facilitated fuel dispersion. In addition to space charge effects, elevated temperature can have a very significant effect on the electro spray structure.

#### 4.1 Electro spray phenomenology at elevated temperature

If the fundamental mechanism of electro spray generation is envisioned as a balance between Coulombic force on the liquid and surface tension, it is evident that the elevated temperatures associated with combustion applications can drastically alter the electro spray phenomenology observed for injection of liquids in “cold” conditions.<sup>11)</sup> This occurs for two reasons: first, the sharp decrease of surface tension near the boiling point; and second, the expected increase with temperature of the fluid electric conductivity, as a result of a decrease in liquid viscosity and the consequent enhancement in ion mobility. Furthermore, the fluid patterns associated with the electro spray usually consist of high surface-to-volume ratio morphologies (cones, elongated cylindrical ligaments), which can be particularly vulnerable to enhanced evaporation of the fluid in hot environments.

To characterize the electro spray phenomenology at temperatures close to the boiling point of the injected fluid, an ethanol (boiling point: 78.5°C) electro spray was established and observed photographically with the use of the second harmonic of a Nd : YAG laser as a fast (5 ns) light source, to freeze the action and a Canon EOS 3 digital camera adapted on a Bausch and Lomb microscope. The ambient temperature was controlled by a slow coflow of heated air around the electro spray capillary. Ethanol was preferred because the fuel boiling point could be reached with modest requirements in heating power. Also, for liquid hydrocarbon surrogates that would simulate logistic fuels, coking could occur and complicate the phenomenon unnecessarily.

Figure 4 shows a “cone-jet” spray that was established at room temperature by charging the capillary to 4.5 kV and using a ground located 2 cm from the tube exit. The ethanol flow rate was 0.5 mL/h. As the electric field was kept constant and the temperature increased, the spray underwent a series of abrupt transformations shown in Fig. 4. At approximately 45°C, the integrity of the cone of Fig. 4a could not be sustained by the decreasing ethanol surface tension. Data from ref. 12 suggest a descending third order polynomial dependence of ethanol surface tension on temperature for the temperatures of interest here. The stable cone broke apart in two significantly smaller unstable cones located diametrically opposite on the capillary tip and spinning around it. Further break-up to multiple cones followed as the temperature increased, with

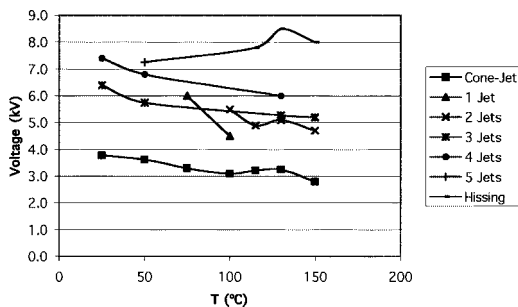


Fig. 5. Onset voltages for several dodecane electro spray regimes.

ever smaller cones located on the vertices of spinning canonical polygons of an increasing number of sides (Figs. 4b and c). The distance between the tube and each spray fan appeared to increase with temperature, probably as a result of space charge interaction among the multiple electro sprays. When the temperature rose very close to the boiling point ( $>70^{\circ}\text{C}$ ), the electro sprays became unstable, in part because of sudden changes in conductivity when the conductive fluid was boiling on the tube rim. The canonical polygonal structures were not observed any longer and they were substituted by a multitude of intermittent sprays. This phenomenon was also accompanied by the emission of a “hissing” sound, which is typically characteristic of the onset of corona discharge.

This phenomenology is very much reminiscent of what occurs at constant temperature as the voltage between capillary and ground is increased.<sup>11)</sup> This is not surprising since one can affect on the balance of electric “disruptive forces” and surface tension cohesive ones, either by increasing the first or decreasing the latter. The onset voltage for the various regimes is shown as a function of temperature in Fig. 5 for an *n*-dodecane (boiling point: 216°C) electro spray at a flow rate of 1.0 mL/h. The trends described above pertain qualitatively with the onset voltages for multicone formations dropping in general with temperature. It should be noted that the temperatures here are significantly lower than the boiling point, unlike the ethanol case. For this reason, there is a relatively “broad” cone-jet regime before multiple cones appear. As the ambient temperature is elevated closer to the boiling point, the situation appears more complicated with the onset curves of the various regimes overlapping. The situation for heavy, liquid hydrocarbon fuels may also be complicated by coke formation in the capillary.

The implications of these results with respect to the operation of mesoscale power generation devices based on electro spray liquid fuel injection are important, since they indicate that a balance has to be achieved between two desirable but conflicting characteristics of burner:

- i. Operation in the well defined “cone jet mode” which will yield monodisperse sprays and well characterized vaporization times; and
- ii. Extensive heat recuperation, that can in principle improve the thermodynamic efficiency of such devices, an expectation though that may not be achieved because of poor spray quality and subsequent mixing.

The degree within which such a balance can be achieved was studied using laser diagnostics. The results will be eventually complemented with droplet size measurements, which will further characterize the quality of the involved electro sprays.

#### 4.2 PLIF images of spray modes

Figure 6 shows a series of time-averaged (100 laser shots) and a series of single-shot images taken at a location in the evaporation chamber such that the laser sheet was intersecting the axis of two of the 19 sprays. Virtually the entire height of the chamber is imaged, with the exception of a 1–1.5 mm strip.

In each series, images from operation at 0 kV, 6 kV,

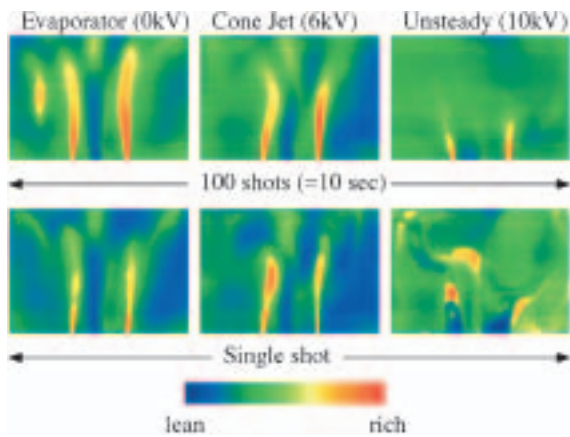


Fig. 6. Time-averaged and single-shot PLIF images of the sprays in different operatin modes.

and 10 kV electric potential between needle and catalyst are shown. Without voltage, the needles operate as evaporators, which is sustainable because of the intake air heating and the back radiation from the catalyst grid. The single-shot image is essentially identical (apart from intensity and noise) to the time-averaged one, except for the small fluctuations caused by the stepper motor of the syringe pump. The partial recirculation of fuel vapor downwards along the left and right window, caused by the fact that not the entire chamber bottom has intake holes, can also be seen. Temperature measurements for these conditions with the infrared camera indicate that the temperature distribution on the catalyst is very inhomogeneous with a “spotty” pattern of hot reaction regions surrounded by cold, non operating parts of the catalyst. Apparently, liquid evaporation and diffusion in the gaseous phase is not an effective mechanism for fuel dispersion and mixing. This mode of operation is also very unfavorable because the needles coke quickly.

When the capillaries are charged at 6 kV, most of the sprays operate in a stable cone-jet mode. Again, single-shot and time-averaged images look similar. The recirculation pattern cannot be seen as clearly anymore. Catalyst uniformity is improved because of the liquid dispersion due to the Coulombic force. When the voltage is increased further, the cone-jet mode becomes unstable for most sprays and the “hissing sound” mode described in the previous section is established. It is now particularly interesting to compare single shot and average images: the time-averaged image shows a more homogenous mixture throughout the field and a shorter zone of nearly unmixed fuel, whereas the single-shot image reveals a completely unsteady structure comprised of fuel-rich eddies that are not necessarily where the richest mixture is found on average. PLIF does not provide any velocity information, but in view of mushroom-shaped rich eddies that can be seen on some of the single-shot images (not shown here) it is suggested that a highly unsteady flow field is established throughout the chamber, contrary to the intuitive image of a smooth laminar flow pattern. The source of unsteadiness is attributed to the irregular emission of droplets from the capillaries. Clearly mixing is enhanced strongly in this unsteady mode of

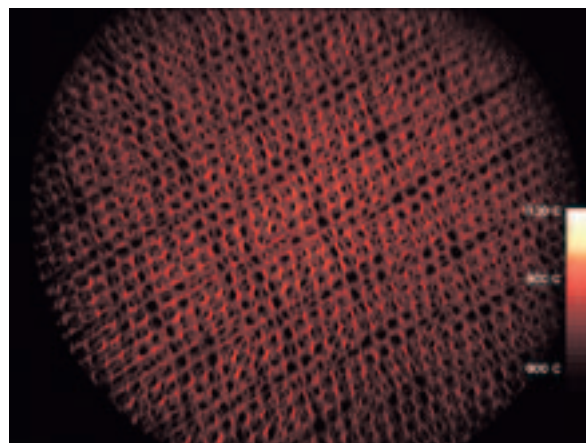


Fig. 7. Two-dimensional map of temperature on the catalytic screen acquired with infrared photography.

operation. The catalyst temperature and visual appearance are very uniform. An infrared thermographic image is shown in Fig. 7 indicating a  $\pm 5\%$  uniformity across the catalytic grid. The currently unstudied “hissing sound” mode seems to be preferable for the operation of the particular burner.

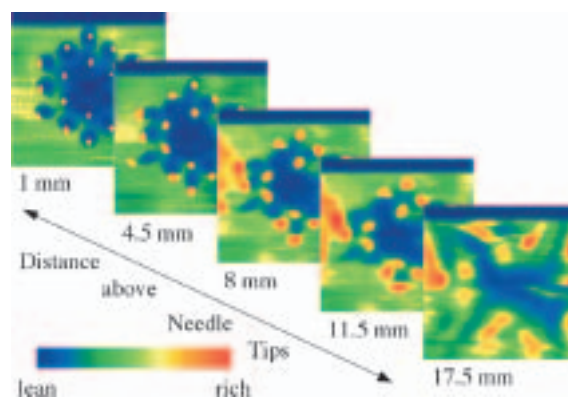


Fig. 8. Mixing patterns in chamber cross-sections parallel to the catalyst, as obtained from a 3D reconstruction of the PLIF measurements for the case of 0 kV.

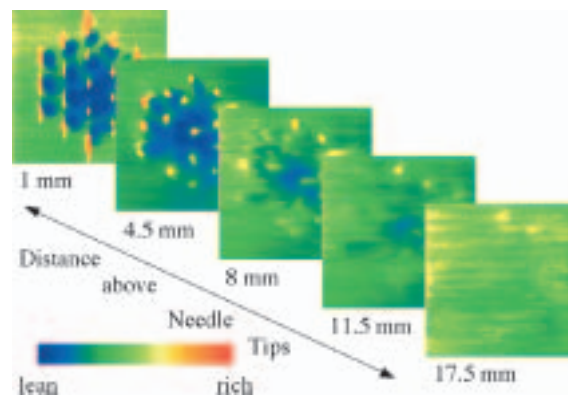


Fig. 9. Mixing patterns in chamber cross-sections parallel to the catalyst, as obtained from a 3D reconstruction of the PLIF measurements for the case of 10 kV.

### 4.3 3D-Reconstruction of fuel dispersion

Since time-averaged images, even in the unsteady, “hissing sound” mode, are relatively stable, it is possible to reconstruct the information throughout the entire chamber by scanning in the third dimension, perpendicular to the catalyst grid, and combining the vertical slices obtained. In this way a complete image of the time-averaged, three-dimensional mixing process can be formed. Images are taken in steps of 0.5 mm, to a distance of about 0.5 mm from each wall, giving a total of 58 slices. Figures 8 and 9 each show a series of horizontal slices through the 3D array for the case of 0 and 10 kV applied voltage, respectively. The apparent spatial resolution in the transverse direction was increased by interpolation to have the image proportions match the physical proportions. The dark stripe on the top portion of the 0 kV-series is caused by running out of fuel at the end of the experiment and the corresponding last few images accordingly show zero equivalence ratio.

The lowest slice of both series is similar: the very fuel-rich jets (the false color scale has been saturated significantly here to be able to resolve finer shades in the higher slices on the same scale) are surrounded by pure air from the intake holes. The nature of the stripes extending “vertically” from the jets in Fig. 9 is not clear, despite several experiments aimed at shedding light on this peculiarity. However, they do not extend upwards further than  $\sim 1$  mm. The “horizontal” stripes in all images are caused by fluctuations in laser power over the duration of the scan. In these image series it can very clearly be seen how much mixing is increased by the unsteady spray mode as compared to molecular diffusion in the laminar flow. The uniform mixing upstream of the catalyst suggested by Fig. 9 is in qualitative agreement with the infrared thermography results of Fig. 7.

### 4.4 Combustion efficiency, CO emission

Combustion efficiency and CO emission were studied using n-dodecane as a single component fuel surrogate, for which the related chemistry could be calculated precisely. This is the most abundant liquid hydrocarbon in JP8. For a base case of operation with equivalence ratio  $\phi=0.48$  and a fuel flow rate of 9.7 g/h, gas chromatographic measurements of mole fractions of the main components,  $N_2$ ,  $O_2$ ,  $CO_2$ , and CO, in a dry sample from the exhaust gas yielded 81.5%, 11.5%, 6.4%, 0.11%, respectively. Light hydrocarbons like  $CH_4$  and  $C_2H_6$  as well as  $H_2$  were below the detection threshold of the particular GC apparatus (50 ppm). Also,  $C_2H_2$  and light aromatics, which are generally important in soot formation could not be detected, which indicates that, contrary to virtually all combustion configurations, the current burner achieves diesel fuel combustion without soot formation. On the basis of this data a combustion efficiency of 97% can be estimated.<sup>8)</sup>

A very good measure of combustion efficiency is the  $CO_2/CO$  mole ratio in the exhaust gases, presented in Figs. 10a, b along with the mole fraction of CO in the exhaust gases as a function of operation parameters of the burner.  $CO_2$  is the product of complete combustion. Since we do not detect any significant quantities of

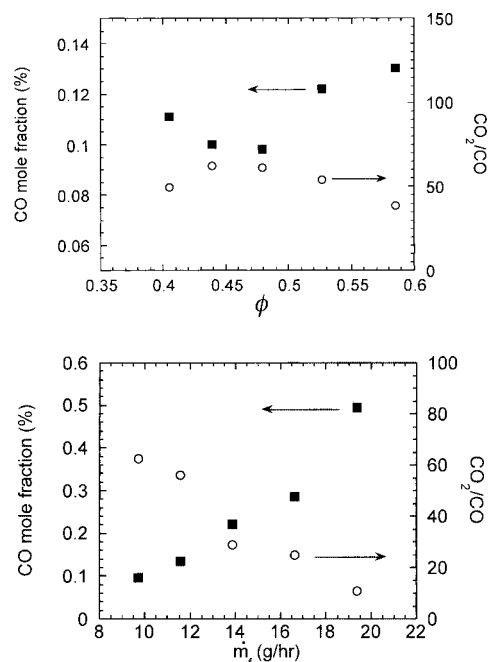


Fig. 10. CO mole fraction (%) and  $CO_2/CO$  ratio on a molar basis ( $\circ$ ) as a function of a) equivalence ratio, for a fixed fuel flow rate of 9.7 g/h, and b) fuel mass flow rate, for a fixed  $\phi=0.48$ .

organics, we can assume that approximately all carbon that has not been completely oxidized is in CO. Moreover CO is a significant pollutant, since its emission may restrict significantly the applicability of such power sources (*e.g.*, for indoor applications).

The high values of the  $CO_2/CO$  ratio indicate a very efficient conversion and reflect the critical importance of catalytic combustion. In Fig. 10a, CO emission is presented as a function of equivalence ratio for a mass flow rate of fuel equal to 9.7 g/h. Since the fuel flow rate was kept constant, the equivalence ratio was varied by changing the air flow. One would expect that proximity to stoichiometric fuel/air proportion would mean higher temperatures and therefore more complete conversion to  $CO_2$ . However, Fig. 10a shows that this is clearly not the case with an optimum conversion achieved for  $\phi \approx 0.48$ . Actually, the operation of the burner is completely suspended for  $\phi > 0.70$  and  $\phi < 0.25$ . This is currently attributed to the fact that variation of the air flow also varies the residence time in the vicinity of the catalyst. Also, careful design of a catalyst specifically tailored for the particular fuel may improve this aspect. For the “optimal” equivalence ratio of ( $\phi=0.48$ , CO to  $CO_2$  conversion is presented as a function of the fuel mass flow rate in Fig. 10b. Since the equivalence ratio is fixed, fuel flow rate is proportional to total flow rate and inversely proportional to residence time in the burner. As residence time decreases, it is clear that the CO to  $CO_2$  conversion is kinetically more limited and less effective.

## 5. Conclusions

The electrospray application to mesoscale combustion was demonstrated to provide a unique means of dispersing the fuel and mixing it with the oxidizer in small volumes, for subsequent catalytic oxidation.

High combustion efficiencies and uniform combustion temperatures were achieved when the electrospray was operated in an unstable mode, accompanied by a hissing sound characteristic of the onset of corona discharge. Laser-induced fluorescence proved to be a very useful tool to image the spray phenomenology in confined environments.

### References

- 1) A. H. Lefebvre, "Atomization and Sprays," Hemisphere (1989).
- 2) M. Cloupeau and B. Prunet-Foch, *J. Electrostat.*, **25** (1990), 165.
- 3) K. Tang, Ph.D. Thesis, Yale University (1994).
- 4) K. C. Thong and F. J. Weinberg, *Proc. Roy. Soc. Lond.*, **324**, 201 (1971).
- 5) G. Chen and A. Gomez, "Counterflow Diffusion Flames of Quasi-Monodisperse Electrostatic Sprays," 24th Symposium (International) on Combustion (1992), pp. 1531–1539; see, also, A. Gomez and G. Chen, *Combust. Sci. and Tech.*, **96**, 47 (1994).
- 6) T. Edwards and L. Q. Maurice, *J. Prop. & Power*, **17**, 461 (2001).
- 7) US Patent No. 5,051,241, William C. Pfefferle (Precision Combustion, Inc.), 1991.
- 8) D. C. Kyritsis, I. Guerrero-Arias, S. Roychoudhury, and A. Gomez, *Proc. Combust. Inst.*, to appear (2002).
- 9) A. C. Eckbreth, "Laser Diagnostics for Combustion and Species," Gordon and Breach, Amsterdam (1996).
- 10) J. Reboux *et al.*, Study of Mixture Inhomogeneities and Combustion Development in an S.I. Engine Using a New Approach of Laser Induced Fluorescence (FARLIF), SAE Tech. Pap. Ser. 961205 (1996).
- 11) K. Tang and A. Gomez, *J. Colloid & Interface Sci.*, **184**, 500 (1996).
- 12) "The CRC Handbook of Chemistry and Physics," 75th Ed., CRC Press, London (1994).

**Keywords:** Electrospray, Combustion, Mesoscale, Fluorescence, Hydrocarbons